Original Article

A novel mesenchymal epithelial transition (MET) inhibitor, CB538, relieves acquired resistance in *EGFR*-mutated *MET*-amplified non-small cell lung cancer

Ji Yeon Song[1,2]^, Hyunsook An[1], Soojeong Kim[1]

[1]CHA (Christianity, Humanism and Academia) Advanced Research Institute, Seongnam-si, Korea; [2]College of Pharmacy, CHA (Christianity, Humanism and Academia) University, Pocheon, Korea

Contributions: (I) Conception and design: JY Song, H An; (II) Administrative support: All authors; (III) Provision of study materials or patients: H An, S Kim; (IV) Collection and assembly of data: JY Song; (V) Data analysis and interpretation: JY Song; (VI) Manuscript writing: All authors; (VII) Final approval of manuscript: All authors.

Correspondence to: Ji Yeon Song, PhD. Candidate, CHA (Christianity, Humanism and Academia) Advanced Research Institute, 335 Pangyo-ro, Bundang-gu, Seongnam-si, Gyeonggi-do 13488, Korea; College of Pharmacy, CHA (Christianity, Humanism and Academia) University, Pocheon, Korea. Email: hisong2283@chamc.co.kr.

Background: Osimertinib, a third-generation epidermal growth factor receptor (EGFR) tyrosine kinase inhibitor (TKI), is the first-line standard therapy for metastatic *EGFR*-mutated non-small cell lung cancer (NSCLC). Although osimertinib is effective, it's durable response is invariably limited by the emergence of acquired resistance. Mesenchymal epithelial transition (*MET*) amplification is a frequent mechanism in patients with *EGFR*-mutated NSCLC who are resistant to EGFR-TKIs. Consequently, combined treatment with EGFR-TKIs and MET-TKIs has been explored as a strategy for overcoming this resistance. The current study aimed to explore the single and combination inhibition effect of CB538, a novel MET inhibitor in MET-activated, EGFR-mutant NSCLC cells.

Methods: The cellular inhibitory effects of single and co-treatment of CB538 with EGFR-TKIs were evaluated in the established EGFR-TKI-resistant cells [PC9/ER (erlotinib resistance), HCC827/OR (osimertinib resistance)]. The preclinical activities of CB538 were investigated by evaluating *in vitro* kinase activity, cell growth, and Western blotting of phosphorylated MET and downstream signaling molecules in MET-activated, EGFR-TKI-resistant cells. Cell viability was examined by MTT and colony formation. The inhibition of migration was determined by wound-healing assay. A xenograft tumor model was employed to investigate *in vivo* HCC827/OR cell growth in BALB/c nude mice.

Results: We confirmed that activated MET/Axl signaling pathways and EMT-related proteins were inhibited by CB538 in established EGFR-TKI-resistant NSCLC cells. CB538, a novel c-MET inhibitor, decreased the growth, migration, and invasive properties of these EGFR-TKI-resistant NSCLC cells. CB538 also inhibited tumor growth and expression of activated proteins (MET and Axl) in *in vivo* HCC827/OR xenograft model.

Conclusions: Additional treatment with CB538 enhanced sensitivity to EGFR-TKIs in two EGFR-TKI-resistant NSCLC cells by inhibiting EGFR/MET/Axl pathway axis. Overall, the treatment effects of CB538 were confirmed to relieve EGFR-TKI-driven resistance in *EGFR*-mutant NSCLC cells.

Keywords: Epidermal growth factor receptor tyrosine kinase inhibitor (EGFR-TKI); osimertinib resistance; mesenchymal epithelial transition amplification (*MET* amplification); MET-TKI; *EGFR*-mutant non-small cell lung cancer (*EGFR*-mutant NSCLC)

^ ORCID: 0009-0004-8210-3173.

Submitted Sep 04, 2024. Accepted for publication Jan 03, 2025. Published online Mar 24, 2025.
doi: 10.21037/tcr-24-1614
View this article at: https://dx.doi.org/10.21037/tcr-24-1614

Introduction

Non-small cell lung cancer (NSCLC) is the poor prognosis tumor, accounting for approximately 80–90% of lung cancers. Furthermore, adenocarcinoma is the most frequent histological subtype of NSCLC. *Epidermal growth factor receptor* (*EGFR*) is one of the most common driver genes of NSCLC. *EGFR* mutations display a heterogeneous representation depending on ethnicity and region (1). Treatment of patients with NSCLC harboring *EGFR* tyrosine kinase inhibitor (TKI)-sensitizing mutations using EGFR-TKIs, such as erlotinib or afatinib, as an initial therapy has been shown to extend progression-free survival (PFS) (2,3). However, 50% or more of these patients exhibited disease progression. Recently, third-generation EGFR-TKIs (e.g., osimertinib) have started to represent promising therapeutic options for patients with NSCLC who have become resistant to first- or second-generation EGFR-TKIs because of the emergence of the *EGFR* T790M mutation (4-6) which is a potent and irreversible EGFR-TKI that targets *EGFR* mutations without affecting wild-type *EGFR*. With its remarkable efficacy and affordable safety, osimertinib is recommended as the standard first-line treatment for patients with advanced or metastatic NSCLC harboring *EGFR* mutations. However, resistance to the third-generation EGFR-TKIs has been described previously. Osimertinib-treated patients as first-line treatment tend to develop resistance after 18.9 months of treatment (1,3,6).

Several mechanisms have been related to acquired resistance to EGFR-TKIs (7,8). For osimertinib, these include the development of secondary *EGFR* mutations and activation of bypass signaling pathways. Additionally, mesenchymal epithelial transition (*MET*) amplification, Axl activation, and epithelial-to-mesenchymal transition (EMT) are crucial mechanisms responsible for acquired resistance to EGFR-TKIs. The resistance to TKIs can be involved by the EMT-status and Axl expression. EMT and Axl are associated with reduced sensitivity to many chemotherapeutic and anticancer drugs (9-13). *MET* amplification is a cause of the most common EGFR-independent mechanism of osimertinib resistance, accounting for 5–24% (6,14,15). Activation of the hepatocyte growth factor (HGF)/c-Met pathway provides a powerful signal for cell proliferation, survival, migration, invasion, and angiogenesis (16-18). A clinical trial on osimertinib combined with crizotinib, initially developed as a MET inhibitor, was also studied in a retrospective analysis, which showed that the overall response rate (ORR) was 100% and the median PFS was 6.2 months in patients with lung adenocarcinoma with *MET* amplification (17,19). Approved MET inhibitor, Tepotinib (Tepmetko®) and EGFR-TKI, osimertinib (Tagrisso®) are promising combinations for patients with osimertinib-pretreated, *EGFR*-mutated, *MET*-amplified NSCLC. Tepotinib plus osimertinib revealed an ORR of 45.8% [95% confidence interval (CI), 31.4–60.8%] in patients with *MET* amplificated NSCLC from phase 2 INSIGHT 2 trial (NCT03940703) (20).

Thus, simultaneous inhibition of both EGFR and MET is required to overcome resistance to EGFR inhibitors following

Highlight box

Key findings

- CB538 inhibited the colony formation and migration in mesenchymal epithelial transition (MET) activated, epithelial growth factor receptor (EGFR)-tyrosine kinase inhibitor (TKI)-resistant non-small cell lung cancer (NSCLC) cells.
- CB538 exhibited a similar inhibition efficacy than the clinically available MET inhibitor, capmatinib, on migration and invasion of MET-activated, EGFR-TKI-resistant cell lines.

What is known and what is new?

- Concomitant treatment of MET inhibitor with osimertinib is known to have potential to overcome drug resistance in EGFR-TKI-resistant NSCLC cells with *EGFR* mutation and *MET* gene amplification. However, single treatment of MET inhibitor, CB538, was as effective as a combination treatment in MET-activated, EGFR-TKI-resistant NSCLCs in this study.
- Crosstalk between MET and Axl has been reported in several cancer cells. New findings confirmed that MET knockdown inhibited the expression of Axl as well as MET in EGFR mutant NSCLC cells (erlotinib-resistant PC9, osimertinib-resistant HCC827 cells).

What is the implication and should change now?

- More selective and potential MET inhibitors, including CB538, could be the treatment option to overcome EGFR-TKI resistant NSCLC.

MET amplification (19-22). We evaluated CB538 as a type II MET-TKI in MET-activated, EGFR-TKI-resistant NSCLCs because of its potent inhibitory efficacy against c-Met-activated cancer cells and MET mutant kinases. In this study, we determined that MET activation is a key mechanism in acquired resistance to the first- and third-generation EGFR-TKIs, erlotinib, and osimertinib. We further demonstrated that additional treatment of the CB538 MET TKI to EGFR-TKIs could be the option for overcoming the resistance exhibited by EGFR-TKIs-resistant NSCLC cells. We present this article in accordance with the MDAR and ARRIVE reporting checklists (available at https://tcr.amegroups.com/article/view/10.21037/tcr-24-1614/rc).

Methods

Chemicals and reagents

Erlotinib was obtained from Selleckchem (Houston, TX, USA), and osimertinib and capmatinib were purchased from Combi-Blocks, Inc. (San Diego, CA, USA) and MedChemExpress (Monmouth, NJ, USA), respectively. CB538 (MW. 687.7) was provided by CMG Pharmaceutical, Co., Ltd. (Seongnam City, Korea). Other chemicals were used from Sigma-Aldrich (St. Louis, MO, USA). Dimethyl sulfoxide (DMSO) was used as a vehicle solvent for *in vitro* experiments and stored at –20 ℃.

Kinase inhibition assay

The ADP (adenocine diphosphate)-Glo™ luminescent kinase assay kit (Promega, Madison, WI, USA) was used to monitor an *in vitro* kinase activity assay. The 50% inhibition concentration (IC_{50}) of c-Met inhibition potency by compounds was evaluated under 10 μmol/L adenocine triphosphate (ATP) using recombinant human c-Met protein. The compounds were diluted 10-fold, and 10 μL kinase reactions were performed in 384-well plates at room temperature (RT) for 1 h. ADP-Glo™ reagent (5 μL) was added to stop the kinase reaction. After the Kinase Detection Reagent was added, the ADP-Glo™ Kinase Assay luminescence generated by the luciferase/luciferin reaction was measured, and a titration curve was generated using a luminometer (GloMax® Discover, Promega). Kinase selectivity profiling was conducted at the Eurofins Pharma Discovery Services (Dundee, UK) according to their manufacturer's instructions. The inhibitory effect of CB538 on 60 kinases was evaluated by a concentration of 500 nM at the K_m of ATP and expressed as a percentage inhibition.

Cell culture and reagents

Human NSCLC cell line, PC-9 was gifted from Dr. Byoung Chul Cho lab (Yonsei Univ College of Medicine, Seoul, Korea), and HCC827 cell (#CRL-2868) was obtained from ATCC (Rockville, MD, USA). EGFR-TKI-resistant cells, erlotinib-resistant PC-9/ER, and osimertinib-resistant HCC827/OR cells were generated by culturing parental cells with escalating doses of EGFR-TKIs. Parental PC-9 and HCC827 cells were exposed to increasing concentrations of each compound, starting at 0.01 μM (IC_{50} values). Cells were treated from 0.01 to 10 μM, and drug concentrations were increased 5-fold. The resistant cells were exposed to concentrations of at least 1 μM for a few months. All cell lines were cultured in RPMI media (Gibco, USA) supplemented with 10% heat-inactivated fetal bovine serum (FBS, Gibco, Waltham, MA, USA) and 1% antibiotics-antimycotics. Recombinant hHGF was manufactured from R&D Systems (#294-HGN-025, Minnesota, USA).

Cell proliferation assay

Cells were seeded at 1,500 cells/well in a white-bottom 384-well plate (Corning, NY, USA) (n=3) and treated with dose-escalated compounds at 37 ℃ in an atmosphere containing 5% CO_2 for 72–96 h. Cell growth was assessed by a Cell Titer-Glo® (Promega) assay. The 0.5% DMSO treated cell groups were set as 100% positive control. The IC_{50} values were calculated by fitting the concentration-response curve using four-parameter analytical methods (GraphPad Software, Inc., version 9.5.1) (La Jolla, CA, USA).

Colony-forming assay

The cells were seeded in 6-well plates at a density of 2,000 cells per well. After overnight incubation, the cells were cultured for 12–15 days. The drugs were changed every 3 days. The 0.5% DMSO treated cell groups were set as 100% positive control. Then, cells were stained with crystal violet for 20 min and counted using the ImageJ software (NIH, Bethesda, MP, USA).

Cell invasion and wound healing assay

The CytoSelect™ 24-well cell invasion assay was performed

using 8 μm pore size Boyden chamber plates (Cell Biolabs, San Diego, CA, USA) as a manufacturer's instructions. Briefly, the cells were incubated in a serum-free medium for 24 h, and the cell suspension (5×10^5 cells) was plated in the upper chamber. Serum-free medium containing 100 ng/mL HGF was then added to the lower chamber. For compound treatments, 0.5 μM of erlotinib, osimertinib, and 0.1 μM of CB538, capmatinib were added to the upper chambers. The isolated upper chamber was washed to remove noninvasive cells and stained with CyQUANT colorimetric dye. Using an enzyme-linked immunosorbent assay (ELISA) reader, the solution obtained by dissolving stained cells in 1% acetic acid was measured at 560 nm. For the wound healing assay, cells (1×10^6 cells/well) were cultured in a 6-well plate. A wound in a confluent monolayer was scratched with a 200 μL pipette tip and washed with phosphate buffed saline (PBS) to remove non-adherent cells. The cells were immediately treated with the indicated compounds. The 0.5% DMSO treated cell groups were set as 100% positive control. The migration of wound-bordering cells is monitored at 0 h and 24–48 h using a light microscope. The relative variation in the wound area was analyzed using the ImageJ software (n=3). We performed as follows: CBA-100-C-cell-migration-invasion-assay.pdf (https://www.cellbiolab.com/sites/default/CBA-100-C-cell-migration-invasion-assay.pdf).

Gene knockdown by siRNA transfection

The siRNAs were purchased from Dharmacon (Lafayett, Colorado, USA). The negative control siRNA was acquired from Bioneer (SN-1011, Daejeon-si, Korea). Briefly, cells were seeded in 6-well plates (1×10^6 cells/mL) 1 day before transfection with growth medium without antibiotics to ensure a confluency of 30–50% was reached by the time of transfection.

For each transfection sample, the transfection complex was prepared by diluting 500 pmol of siRNA oligomer and 9 μL of Lipofectamine™ RNAiMAX (Invitrogen, Carlsbad, CA, USA) with 250 μL of Opti-MEM (Thermo Fisher Scientific, Inc., Waltham, MA, USA) without serum, which was added to each well in the cell seeding plate. We experimented with the previously described method: after incubation in a CO_2 incubator at 37 ℃ for 24 h, the medium containing siRNA and transfection agent was replaced with fresh medium. To confirm that the expression levels of the target proteins were downregulated, cells were collected and lysed 48 h after transfection for western blotting. A protocol was prepared before the study without registration. The siRNA sequences against MET (D-003156, Dharmacon) were as follows: GAACAGAAUCACUGACAUA and GAAACUGUAUGCUGGAUGA.

Immunoprecipitation (IP) and immunoblot analyses

Cells were serum-starved overnight and stimulated with or without HGF (100 ng/mL) for 10 min. Protein lysates were extracted with the a Cell Signaling Technology (Beverly, MA, USA) lysis buffer. The lysates were quantified using a bicinchoninic acid (BCA) protein assay (R&D Systems). Cell lysates (100–200 ng/well) were incubated with the indicated antibodies for IP, and the immune complexes were incubated at 25 ℃ for 1 h. A protocol was prepared before the study without registration. Immune complexes were reacted with Protein A/G Sepharose beads ina Dynabeads® IP Kit (Thermo Fisher Scientific, Inc.) for 1 h, the beads were washed three times with lysis buffer, and the bound proteins were analyzed by sodium dodecyl sulfate-polyacrylamide gel electrophoresis (SDS-PAGE) and transferred to polyvinylidene difluoride (PVDF) membranes for immunoblotting. After washing three times, the membranes were incubated in a blocking solution [5% bovine serum albumin (BSA)] at RT, followed by incubation with primary antibodies at 4 ℃ overnight. All primary antibodies, except the anti-transforming growth factor (TGF)-β antibody, were purchased from Cell Signaling Technology: anti-pEGFR (#2234), anti-EGFR (#4267) anti-pMET (#3077), anti-MET (#8198), anti-pAKT (#9275), anti-AKT (#4691), anti-pERK (extracellular signal-regulated kinase) (#9101), anti-ERK (#9107), anti-E-cadherin (#14472), anti-N-cadherin (#13116), anti-vimentin (#5741), anti-cleaved PARP (poly (ADP-ribose) polymerase, #9541) and anti-β-actin (#4967). Membranes were then incubated with horseradish peroxidase (HRP)-conjugated secondary antibodies (1:1,000 dilution) at RT for 2 h. Protein bands were visualized using a Chemiluminescence imaging system (W1015, Promega). We used pre-stained protein molecular weight standards. Imaging for immunoblotting was performed using Bio-Imager (GE, Chicago, IL, USA).

Tumor xenograft study

Athymic BALB/c nu/nu mice (NMRI-*Foxn1*$^{nu/nu}$ from Envigo (Indianapolis, IN, USA); male, 4 weeks old, koatech, Korea) were acclimatized for 1 week before the experiment. As reported previously (8), HCC827/OR (5×10^6 cells) cells. and Matrigel (Corning, Bedford, MA, USA) were mixed and prepared immediately in 100

μL PBS before being injected subcutaneously into the left flank of the mice. When the tumor volume reached a volume of 60–80 mm^3, the mice were randomized into the vehicle control and treatment groups (n=5). The vehicle [polyethylene glycol (PEG)300:DMSO:Tween 80:saline solution at a ratio of 40:10:5:45, respectively] was used for the drug treatment solution. Each compound was administrated orally once a day, five times a week for 22 days. Body weight and tumor volumes were measured twice a week. The tumor volumes were measured using a digital slide caliper, and volumes (V; mm^3) were calculated as follows: $V=0.5 \times \text{length} \times \text{width}^2$. At the termination of the experiment, all mice (n=20) were euthanized. All animal experiments were performed with the approval of the Institutional Animal Care and Use Committee Guidelines of CHA (Christianity Humanism Academia) University (IACUC220188, Seongnam, Korea) and in conformity with the National Guidelines for the Care and Use of Laboratory Animals.

Immunohistochemistry staining

Tumors were extracted and chapped at the end of the xenograft experiment. Formalin-fixed paraffin-embedded tumor samples were obtained and deparaffinised. After rehydration in alcohol, immunohistochemical staining for MET and Ki-67 was performed using specified antibodies (Cell Signaling Technologies) against pMET (#3077), MET (#8198), and Ki-67 (#9449). The following day, the sections were washed in PBS, three times and then incubated with anti-rabbit and anti-mouse secondary antibodies (HRP-conjugated) at RT for 2 h. All sections were stained with hematoxylin and eosin.

Statistical analysis

Statistical analyses were performed using GraphPad Prism 7 (GraphPad Software, Inc.). Statistical significance was analyzed using Student's t-test and one-way analysis of variance (ANOVA), and data showed mean ± standard deviation (SD). Statistical significance was set at $P<0.05$.

Results

Establishment of EGFR-TKI-resistant cells

Using the dose-escalation method, we established EGFR-TKI-resistant, *EGFR*-mutant NSCLC cells (PC-9/ER, erlotinib-resistant cells; HCC827/OR, osimertinib-resistant cells). Each EGFR-TKI (erlotinib, osimertinib) was sensitive in parent cells [growth inhibition (GI_{50}) <50 nM], but the established cells showed resistance to each compound, erlotinib/osimertinib, using a drug concentration of 1 μM. We measured the resistance to EGFR-TKIs in PC-9/ER and HCC827/OR using cell viability assays (erlotinib GI_{50} in PC-9/ER, 3.60 μM; osimertinib GI_{50} in HCC827/OR, 2.0 μM; *Figure 1A*). HCC827/OR cells were sensitive to MET inhibitors (GI_{50} <0.5 μM). A single treatment of either MET inhibitor did not inhibit cell growth in PC-9/ER cells, which differed from HCC827/OR cells. However, the combination of the EGFR-TKI and the MET inhibitors effectively inhibited the growth of resistant cells (PC-9/ER, HCC827/OR). As shown in *Figure 1B*, combinatory cell growth inhibition effect by the MET inhibitor and EGFR-TKI in these cell lines demonstrated a GI_{50} value below 0.2 μM (capmatinib, CB538 IC_{50} in PC-9/ER, 0.020, 0.173 μM; capmatinib, CB538 IC_{50} in HCC827/OR, <0.010 μM). HCC827/OR cells had a more fibroblast-like cell shape than parent cells on a light microscope. The round shape of the parental cells changed to a smaller size, and the spindle formed was similar to that of fibroblast cells, suggesting that EMT-like changes might have occurred (*Figure 1C*). Next, we examined the effects of each EGFR-TKI on the EGFR/MET signaling pathway in the PC-9/ER and HCC827/OR clones. Yang *et al.* previously confirmed that the MET downstream signaling pathway was activated by *MET* amplification and Axl upregulation in these cell lines compared with the parent cell lines that harbor the *EGFR* exon 19 deletion (19del) mutation (23). We also observed that MET/Axl signaling pathways were activated in these cells, especially HCC827/OR. Moreover, only a slight reduction in AKT/ERK signaling was observed in resistant cells after administration of low dose EGFR-TKI, erlotinib or osimertinib (*Figure 1D*). To confirm the induction of EMT in PC-9/ER and HCC827/OR cells, we analyzed the expression of EMT-related marker proteins. E-cadherin maintains cell adherence and tight-junction as an epithelial marker, whereas the mesenchymal counterparts are frequently expressed by N-cadherin, fibronectin and vimentin (13). Compared to the parent cells, the expressions of N-cadherin and vimentin were increased in both resistant cell lines, whereas the expression of E-cadherin was reduced in HCC827/OR cells (*Figure 1D*).

Treatment of CB538 relieves acquired resistance to EGFR-TKI

Next, we determined whether adding a MET inhibitor

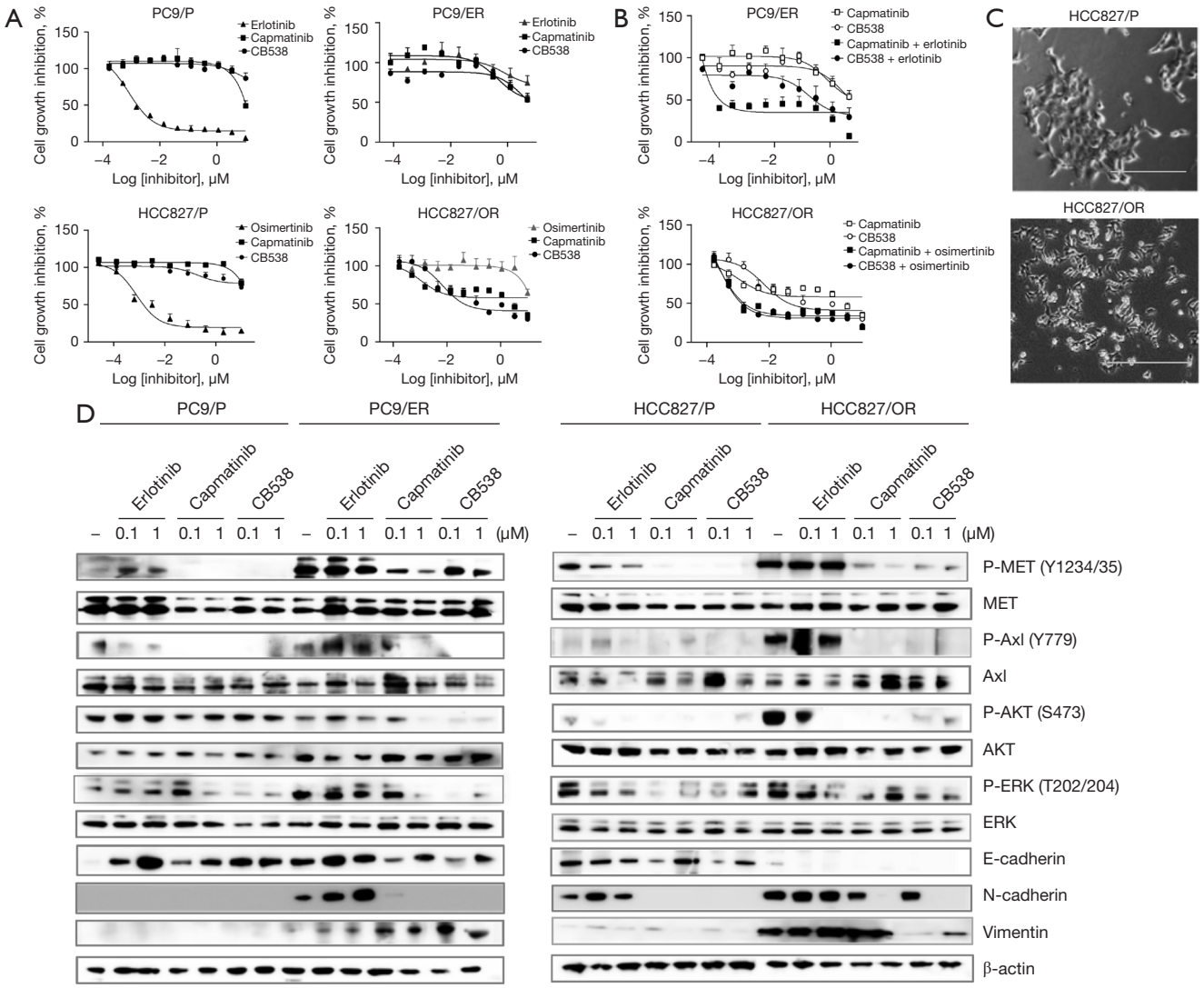

Figure 1 *In vitro* characterization of established EGFR-TKI-resistant cells. (A) Cell viability of MET inhibitors and erlotinib/ osimertinib on parent and resistant cells were analyzed using a MTT assay (n=3). Cell viability was measured after single treatment of CB538 and erlotinib or osimertinib for 72 h in parent cells (PC9, HCC827) and resistant cells (PC9/ER and HCC827/OR). (B) Cell growth inhibition effect by combination treatment of MET inhibitor and EGFR-TKI was analyzed. (C) Morphological differences between parental HCC827 and HCC827/OR cells were observed by optical microscope (1,000 μm scale). (D) The cellular signaling proteins were measured in parent and resistant cells and inhibition effects of single drug treatment were accessed using western blot. Parent and resistant cells were treated with MET-TKI and EGFR-TKI (0.1, 1 μM) in PC9 and HCC827 cells for 4 h, respectively. EGFR, epithelial growth factor receptor; MET, mesenchymal epithelial transition; MTT, 3-(4,5-dimethylthiazol-2-yl)2-,5-diphenyltetrazolium bromide; PC9/ER, erlotinib-resistant PC9; PC9/P, parental PC9; HCC827/OR, osimertinib-resistant HCC827; HCC827/P, parental HCC827; TKI, tyrosine kinase inhibitor.

would relieve EGFR-TKI resistance in EGFR-TKI-resistant cells. We evaluated the effect of CB538, a c-MET inhibitor, on acquired EGFR-TKI resistance in erlotinib-resistant or osimertinib-resistant cells. Furthermore, capmatinib was used as a reference c-MET inhibitor. CB538 showed a selective kinase inhibition profile including Axl, Ron and Mer kinase in many tyrosine kinases besides MET (Table S1). As a selective type II MET inhibitor, CB538 inhibited MET wild type and mutant types (exon 14 skipping, D1228X and Y1230H) (Table S2).

Therefore, we investigated the inhibitory effects of MET inhibitors (capmatinib, CB538) and erlotinib/osimertinib in PC-9/ER and HCC827/OR cells, either as a single or combined treatment. Combination treatment of MET inhibitor and EGFR-TKI showed better inhibitory effects than single treatment in these cells, as shown in *Figure 1B*. Moreover, treatment with a single MET inhibitor and co-treatment with EGFR-TKI inhibited MET/Axl protein phosphorylation and the AKT/ERK downstream pathway proteins for 48 h. The changed expression of EMT-associated markers by drug treatment was maintained by 48 h, too. Inhibition effects of activated MET/AKT/ERK, N-cadherin and vimentin were similar in both single MET inhibitors (*Figure 2A*). Co-treatment of CB538 with EGFR-TKI resulted in better consistent inhibition of EGFR and MET protein in PC-9/ER and HCC827/OR cells for 48 h compared to capmatinib. The inhibitory effect of CB538 in each cell line was further confirmed using a colony formation assay that is already in use. MET-TKI inhibited the colony formation in both PC9/ER and HCC827/OR cell lines. Concurrent treatment of an EGFR-TKI and MET inhibitor resulted in enhanced inhibition of colony formation in PC-9/ER cells compared with a single treatment using either agent alone. MET inhibitor showed the dramatic inhibition effects in HCC827/OR cells (*Figure 2B*). Next, we examined the migratory and invasive potentials, which are considered functional hallmarks of EMT. Using a wound healing assay, we detected the effects of MET inhibitor and EGFR-TKI on cell migration. PC-9/ER and HCC827/OR cells started migrating and closed the wound after 24–48 h. Compared to the control, single treatment and co-treatment of CB538 with erlotinib or osimertinib significantly prevented cell migration (*Figure 2C*). CB538 showed a greater inhibitory effect on cell migration than capmatinib in PC9/ER cells. The inhibitory effects of colony forming and migration of the MET inhibitor were more significant in HCC827/OR cells, indicating that only a single treatment with MET inhibitor showed a sufficient inhibitory effect. Moreover, we found that a single MET inhibitor and a combination of MET inhibitor and EGFR-TKI inhibited the ability of the cells to invade. Combination effects of the MET inhibitor and EGFR-TKI showed a better significant invasion reduction in the CB538-treated groups in both cell lines (*Figure 2D*). Overall, these findings indicate that EMT induction and MET activation are largely accompanied by the acquisition of resistance to EGFR-TKIs and MET TKIs, including CB538, which sensitize these resistances in PC-9/ER and HCC827/OR cells.

Activation of MET induced a resistance to EGFR-TKI in EGFR-TKI-resistant cells

To investigate whether the inhibition effect of MET inhibitors in EGFR-TKI-resistant cells was conducted by targeting c-MET, we treated PC-9/ER and HCC827/OR cells with a MET-specific siRNA. Subsequent MTT assays showed that downregulation of MET significantly reduced cell growth in these cell lines (*Figure 3A*). Furthermore, MET knockdown cells maintained 70% of their maximum cell growth compared to the normal control groups. Western blot analysis also showed that PC-9/ER and HCC827/OR cells exhibited lower phosphorylation of EGFR and MET downstream signaling proteins following MET knockdown. Next, as determined by Western blotting, MET knockdown inhibited the expression of the EMT-related proteins N-cadherin and vimentin, in all cell lines. In contrast, E-cadherin expression was only increased in PC-9/ER cells, thereby exhibiting a different expression pattern in HCC827/OR cells by MET knockdown (*Figure 3B*). Consequently, MET suppression reduced the invasiveness of both cell lines. Treatment of EGFR-TKI inhibited the cell invasion in PC9/ER cells, compared to control. MET knockdown exhibited significant inhibitory effects, better than the treatment of EGFR-TKI on invasion of both cells. However, the addition of EGFR-TKI didn't show a significant inhibitory effect in MET knockdown groups (*Figure 3C*). Western blot results demonstrated a similar expression pattern of phospho-proteins between MET, Axl and EGFR. Along with MET, Axl is a potential biomarker and therapeutic target for cancer therapy. Therefore, we hypothesized that MET forms clusters and interacts with other receptor kinases in response to HGF. Notably, previous studies have added HGF to serum-starved cancer cells and observed a dynamic change in the distribution of MET proteins on the plasma membrane, along with co-clustering of MET and Axl receptor tyrosine kinases (24,25). We investigated the protein interactions between EGFR, Axl, and MET using a co-IP assay. Here, Axl receptors interacted with MET receptors at the basal level of endogenous proteins, although the interaction between the receptors was noticeably weak in the PC-9/ER cells. HGF stimulation can lead to the strong dimerization of MET and Axl in both resistant cell lines (PC-9/ER, HCC827/OR), whereas their interaction was reduced by drug treatment. The treatment of MET inhibitor reduced

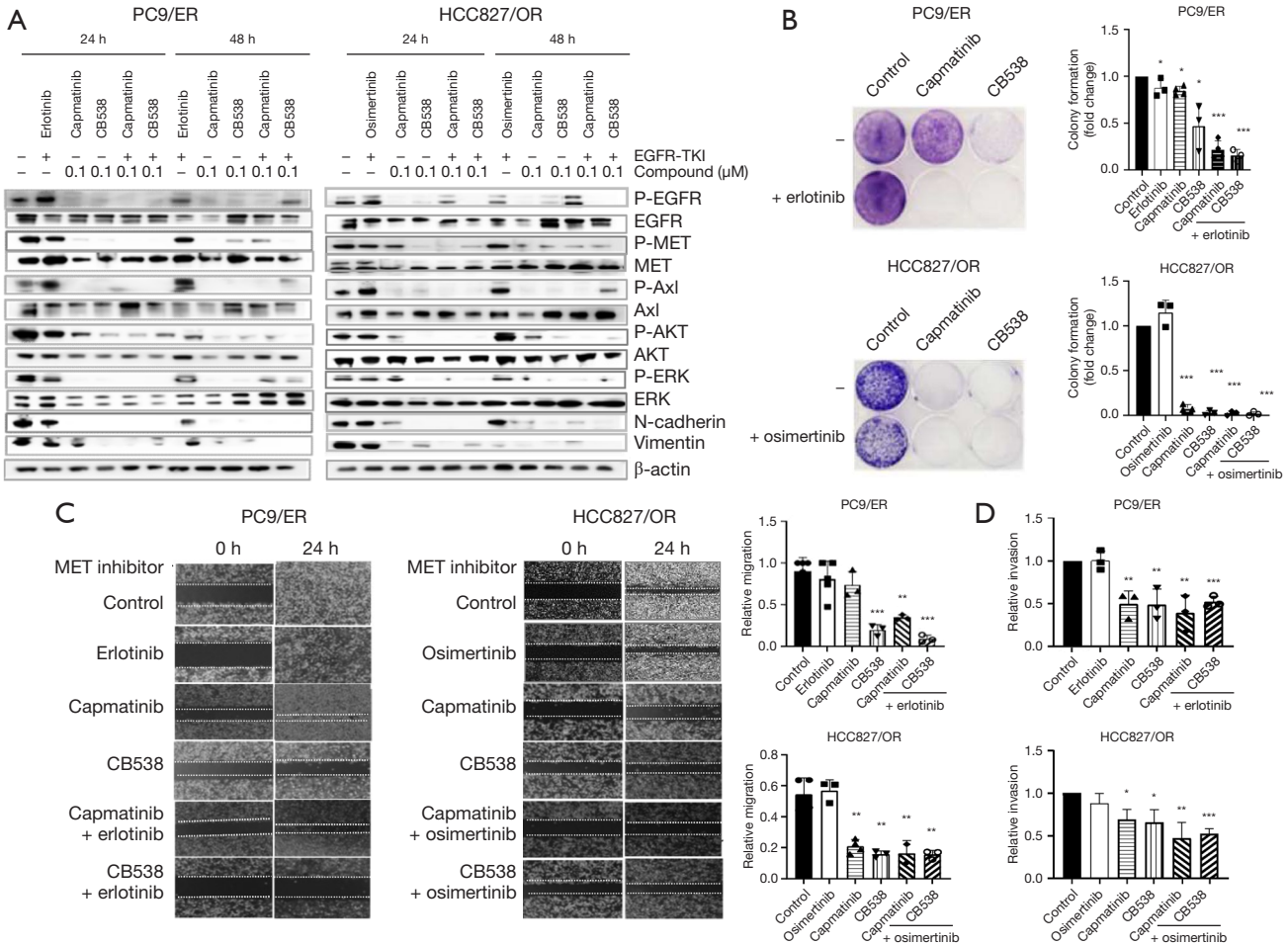

Figure 2 CB538 exhibits anticancer effects on EGFR-TKI resistant cells. (A) The inhibition effects of cellular signaling proteins by single or combination treatment were accessed using western blot. Cells were treated with CB538, Capmatinib (0.1 μM) and/or EGFR-TKI (0.1 μM) in PC9/ER and HCC827/OR cell for 24–48 h. (B) Colony formation assay was used to determine the effects of the concurrent treatment with both compounds in PC9/ER and HCC827/OR cells. Cells were seeded at 2×10^3 cells/mL and treated with compounds every 3 day. After 12–15 days, the culture cell colonies were stained with 0.5% crystal violet and imaged representative images from three separate experiments are shown. (C) The inhibitory effects of cell migration were measured by wound-healing assay. cells were seeded in 6-well plates at 1×10^6 cells/mL and incubated for 24 h. After cells reached 100% confluence, wounds were generated using a 200 μL micropipette tip. After 24–48 h incubation, extents of wound closure areas were measured using ImageJ analysis program. (D) Cell invasion assay was measured by 8-μm pore size Boyden chamber plate. Serum free-culture cells (1×10^6 cells) was seeded on the upper chamber. Serum-free medium containing 100 ng/mL hHGF was placed in the lower chamber. After 48 h, invasive cells at the lower chamber were lysed and dyed. The data shown are the mean ± SD. *, P<0.05; **, P<0.01; ***, P<0.001 *vs.* Control; n=3. EGFR, epithelial growth factor receptor; HGF, hepatocyte growth factor; MET, mesenchymal epithelial transition; PBS, phosphate buffed saline; PC9/ER, erlotinib-resistant PC9; PC9/P, parental PC9; HCC827/OR, osimertinib-resistant HCC827; HCC827/P, parental HCC827; TKI, tyrosine kinase inhibitor.

the interaction of activated MET-Axl in HCC827/OR cells (*Figure 3D*). We observed that treatment with MET siRNA resulted in a concomitant decrease in both MET and Axl expression in PC-9/ER and HCC827/OR cells (*Figure 3B*). We could not confirm the interaction between MET and EGFR in either resistant cell line.

Co-treatment with CB538 and osimertinib reverses acquired osimertinib resistance in vivo

To evaluate the inhibitory effect of CB538 combined with osimertinib on NSCLC cells *in vivo*, a mouse xenograft model was induced subcutaneously by injection of HCC827/OR cells. The drugs were orally administered

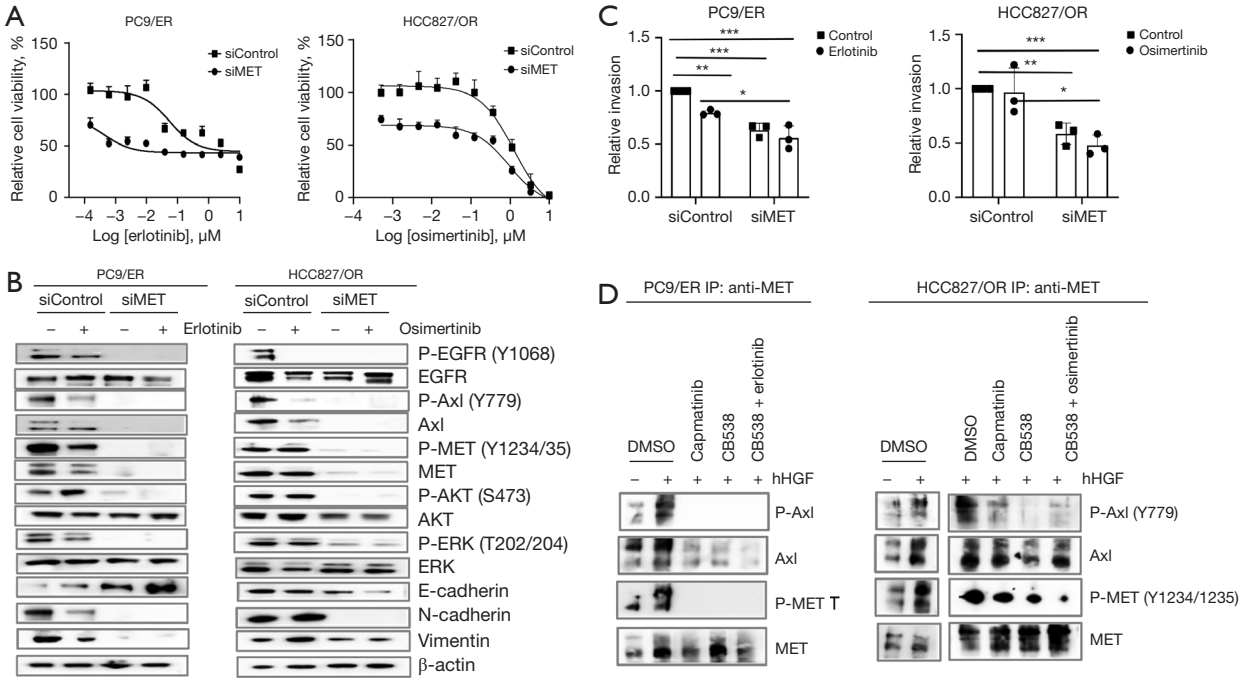

Figure 3 MET signaling pathway mediated the resistance to EGFR-TKI and crosstalk with Axl in PC9/ER and HCC827/OR cells. (A) Cell viability was measured after knocked down by specific siMET in PC9/ER and HCC827/OR. MET knockdown cells were treated with each compound for 72 h. Cell viability was analyzed by MTT assay. (B) The inhibition efficiency of MET knockdown was confirmed by cell signaling pathway using western blot. Cells were treated with MET-specific siRNA for 24–48 h, followed by the treatment with erlotinib or osimertinib for 4 h. The cell lysates were harvested and the phosphorylation of indicated proteins was determined by western blotting. (C) hHGF-induced cell invasion effects in normal (siControl) and MET-knockdown cells (siMET) were measured. Cells were treated with siRNA for 24 h, followed by an additional 24 h of serum starvation. Cells were plated into the upper chambers of Boyden chambers in serum-free medium and with HGF 100 ng/mL in the lower chambers. After 48 h, the invaded cells to the lower chambers were enumerated as described in the Methods. Data was shown as fold difference relative to the vehicle-treated group as mean ± SD. Statistically analysis was performed by one-way ANOVA relative to the control group. *, P<0.05; **, P<0.01; ***, P<0.001 *vs.* Control; n=3. (D) Inhibition of MET-Axl interaction by MET-TKI was confirmed by immunoprecipitation assay. Serum-starved cells were treated with EGFR-TKI, MET-TKI or 0.5% DMSO for 4 h and then with HGF (50 ng/mL) for 10 min. Cell lysates were subjected to IP with anti-MET antibody. The immunocomplexes were western blotted with antibodies specific for Axl (total Axl), P-Axl (Tyr-779-phosphorylated), MET (total MET), and P-MET (Tyr-1234/1235-phosphorylated) as indicated. ANOVA, analysis of variance; DMSO, dimethyl sulfoxide; EGFR, epithelial growth factor receptor; HGF, hepatocyte growth factor; IP, immunoprecipitation; MET, mesenchymal epithelial transition; MTT, 3-(4,5-dimethylthiazol-2-yl)2-,5-diphenyltetrazolium bromide; siControl, negative control; pERK, extracellular signal-regulated kinase; SD, standard deviation; TKI, tyrosine kinase inhibitor; HCC827/OR, osimertinib-resistant HCC827; HCC827/P, parental HCC827; PC9/ER, erlotinib-resistant PC9; PC9/P, parental PC9.

once daily, 5 days per week, for 3 weeks. Treatment with 50 mg/kg CB538 alone or in combination with 5 mg/kg osimertinib led to significant inhibition of tumor growth compared with the saline groups. As shown in *Figure 4A,4B*, single treatment and co-treatment of CB538 with osimertinib significantly inhibited tumor volumes, especially compared to the effect observed in mice treated with osimertinib alone. In addition, we did not observe any body weight loss in mice treated with the inhibitor, either alone or in combination (*Figure 4C*). A few mice in control group showed the maximal body weight reduction of 17% by increasing a rapid tumor size at the end of experiment. The results of immunohistochemistry (*Figure 4D*) for *in vivo* tumor sections showed a decrease in mitotic index (Ki-67), p-MET in CB538 and combination groups. Total and phospho-MET were highly expressed on osimertinib treatment group. Western blotting in tumor lysates significantly decreased the phosphorylation

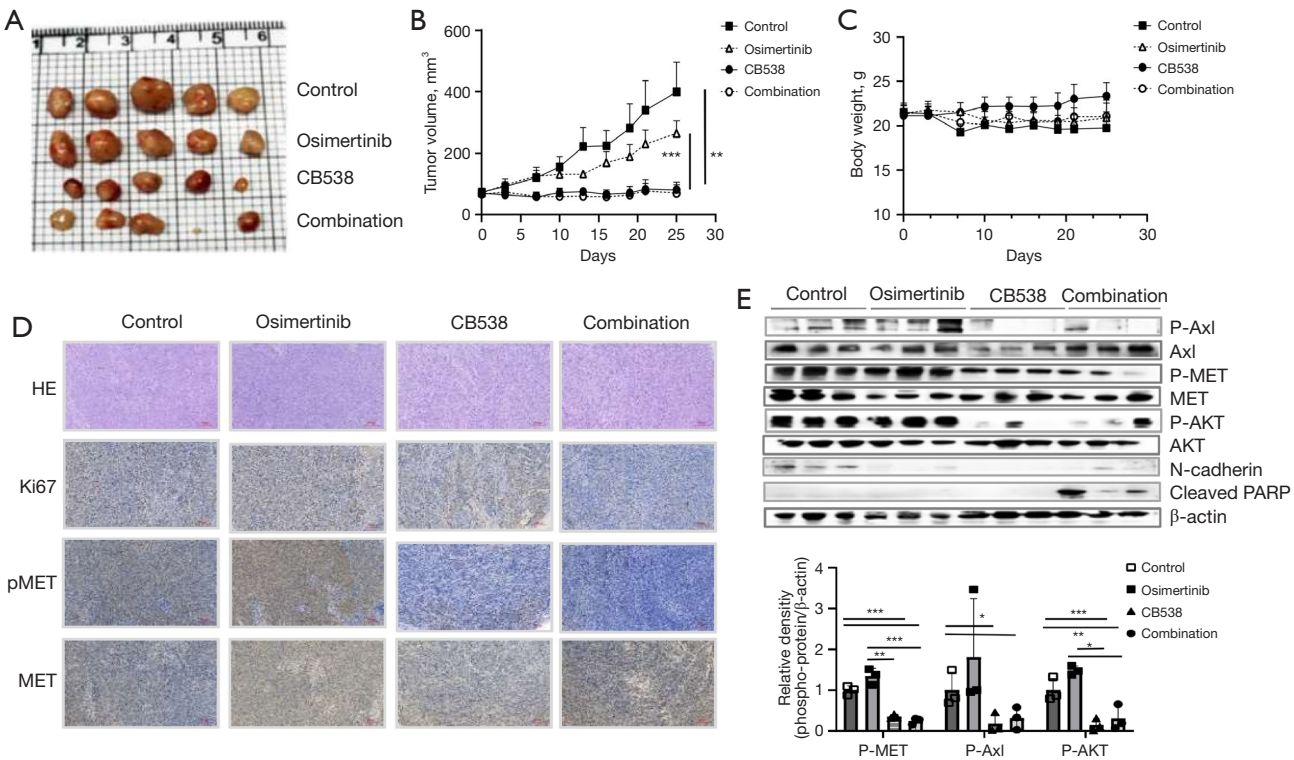

Figure 4 CB538 induced a marked tumor shrinkage to osimertinib-resistant xenograft models harboring HCC827/OR cells. HCC827/OR cells were subcutaneously implanted into athymic BALB/c nu/nu mice. CB538 (50 mg/kg) and osimertinib (5 mg/kg) were given once daily by oral gavage for the indicated period (n=5). After 22 days of each drug treatment, the tumors from two or three mice of each treatment groups were collected. (A) Macroscopic appearance of tumors at the end of experiment. (B,C) The tumor volumes and body weight of mice were measured every 3 days. The results in B and C are indicated as mean ± SD (n=5). (D) The samples were paraffin-embedded and stained with HE or analyzed for immunohistochemistry detection using corresponding antibodies. Scale bars represent 200 μm. (E) Expression of MET, Axl, AKT proteins in *in vivo* xenograft tumors was analyzed using Western blot. Tumor lysates were harvested and the indicated proteins were detected by western blot. Relative protein densities of phospho-proteins were indicated as mean ± SD (n=3). Statistical significance was analyzed by ImageJ and Prism 7.0: *, P<0.05; **, P<0.01; ***, P<0.001 *vs.* Vehicle Control, Osimertinib group. HCC827/OR, osimertinib-resistant HCC827; HE, hematoxylin & eosin; MET, mesenchymal epithelial transition; PARP, poly (ADP-ribose) polymerase; SD, standard deviation.

of MET, Axl and AKT by CB538 and co-treatment with osimertinib. CB538 treatment showed a similar inhibition effect with combination treatment on tumor size, but only combination group enhanced apoptosis-associated protein (cleaved PARP) (*Figure 4E*). We confirmed that apoptosis was induced by combination treatment. Consistent with the *in vitro* experiments, these results suggested that the combined therapy exhibited antitumor effects in HCC827/OR xenograft mice.

Discussion

Despite the mutation and activation of *EGFR* are recognized as important oncogenic drivers in patients with NSCLC, currently existing EGFR-TKIs have shown limited potential due to the emergence of acquired resistance. Recently, osimertinib, a third-generation EGFR-TKI, was reported to have superior efficacy as a first-line treatment targeting the *EGFR* T790M mutation (1). Despite the more potent inhibition of EGFR signaling, patients inescapably develop secondary resistance. The mechanisms underlying resistance to third-generation TKI are complex and not fully understood. *MET* amplification is one of the major resistance mechanisms to osimertinib (5–22%) (7,14). Several preclinical studies and clinical trials have demonstrated that the co-targeting of c-Met inhibitors, such as crizotinib and

tepotinib, with osimertinib has the potential to overcome resistance by *MET* gene amplification in EGFR-TKI-resistant, *EGFR*-mutant NSCLC cell lines (19-22).

To identify the EGFR-TKI resistance mechanism in EGFR-TKI-resistant NSCLC cells, we established erlotinib- or osimertinib-resistant cell lines (PC-9/ER and HCC827/OR) using a dose escalation method for the EGFR-TKI. Compared to EGFR-TKI-sensitive *EGFR*-mutant parent cells, resistant cells were insensitive to growth inhibition induced by EGFR-TKI. A previous study showed that increased activation of MET/Axl and the downstream signaling pathway, AKT/ERK, is associated with acquired resistance to EGFR-TKIs, independent of any additional mutations in *EGFR* (24). Our established resistant cells showed the activation of MET/Axl and AKT/ERK compared to parent cells, especially in HCC827/OR cells. In addition, we found that the expression of EMT-associated proteins (vimentin, N-cadherin) was enhanced.

We investigated the combined anticancer effect of a MET inhibitor and EGFR-TKI and then identified MET activation as a key resistance mechanism to EGFR-TKI. We also evaluated the antitumor effect of CB538, a novel c-MET inhibitor. The results of the present study demonstrated that the MET inhibitors, capmatinib and CB538, re-sensitized erlotinib/osimertinib-resistant NSCLC cells to the EGFR-TKIs. The treatment of a MET inhibitor exerted beneficial effects on the inhibition of cell signaling, viability and colony-forming ability. MET inhibitors alone inhibited the migratory and invasive potential of these cells. We also performed loss-of-function experiments by MET knockdown to demonstrate that MET has an important function in these cells. Notably, *MET*-silencing increased the inhibitory sensitivity toward EGFR-TKI in the established resistant cells. MET silencing inhibited cell signaling downstream proteins (AKT/ERK) and cell viability. MET TKIs also inhibited activated EMT proteins (N-cadherin, vimentin) in EGFR-TKI-resistant NSCLC cells. Some results reported EMT as a candidate mechanism for mediating, especially acquired EGFR-TKI resistance. These *in vitro* observations were confirmed in our mouse model. The mice receiving the CB538 and combination treatment showed tumor reduction effects.

Previous studies have shown that Axl and MET mediate-acquired resistance to EGFR-TKIs and that these receptors regulate metastasis, cell proliferation and poor survival in patients with NSCLC (13,26). Axl is involved in metastasis as an essential regulator of EMT process in cancer cells (27). We also showed that both MET and Axl receptors were activated and interacted via co-IP in EGFR-TKI-resistant cells. Notably, MET knockdown decreased Axl expression, activity of Axl and EMT proteins (N-cadherin, vimentin). Axl and MET signaling share similar downstream molecules, such as PI3K/AKT and MEK/ERK. CB538 treatment reduced the activation of MET/Axl and AKT.

Recent clinical evidence suggests that *MET*-mutation-mediated resistance to type I but not type II MET inhibitors confirmed the potential of sequential use of type I and II inhibitors to achieve a more durable response. Type I MET-TKIs, including crizotinib, capmatinib, tepotinib, and savolitinib, bind to the catalytically active, or DFG-in, conformation of MET where the aspartic acid-phenylalanine-glycine (DFG) motif points into the ATP-binding site. In contrast, type II MET-TKIs, such as cabozantinib, merestinib, and glesatinib, bind to MET in its inactive, or DFG-out state, which competes an additional hydrophobic pocket adjacent to the MET ATP binding site (28,29). Some reports have shown that switching from type I to type II MET inhibitors can delay the resistance driven by *MET* secondary mutations (D1228X, Y1230X) (30-32). Cabozantinib is a multikinase, type II inhibitor with putative preclinical activity against type I MET inhibitor resistance mutations, thereby offering a potential treatment strategy in EGFR-TKI-resistant, MET-activated NSCLC. However, appreciable toxicity has also been reported, which may limit their widespread use (33,34). CB538 is a selective type II inhibitor that inhibits wild-type MET and secondary mutant types. A selective and more potential MET inhibitor should be presented than the current clinical MET inhibitors for sequential use of MET-TKIs.

Conclusions

The present study only analyzed the effects in two EGFR-TKI-resistant cell lines; therefore, further elucidation of the relevant molecular mechanisms is required. However, MET inhibitor, CB538, decreased cell growth, migration, and invasive properties of EGFR-TKI-resistant NSCLC cells. Subsequently, CB538 inhibited tumor cell growth and invasion in single or co-treatment with EGFR-TKIs by inhibiting multiple oncogenic signaling networks, including EGFR, MET, Axl, AKT, and EMT. Thus, the treatment application of CB538 could provide evidence for clinical treatment strategies for patients with *EGFR*-mutant lung cancer.

Acknowledgments

We thank Wonwoo Lee and Heyjin Lee, researchers in CHA advanced research institute, for the technical experimental support in animal study.

Footnote

Reporting Checklist: The authors have completed the MDAR and ARRIVE reporting checklists. Available at https://tcr.amegroups.com/article/view/10.21037/tcr-24-1614/rc

Data Sharing Statement: Available at https://tcr.amegroups.com/article/view/10.21037/tcr-24-1614/dss

Peer Review File: Available at https://tcr.amegroups.com/article/view/10.21037/tcr-24-1614/prf

Funding: This work was supported by an intramural research program from the CHA Advanced Research Institute, Gyeonggi-do, Korea (CARI-RD-034).

Conflicts of Interest: All authors have completed the ICMJE uniform disclosure form (available at https://tcr.amegroups.com/article/view/10.21037/tcr-24-1614/coif). J.Y.S. received funding for provision of study materials and analysis services from CHA Advanced Research institute. J.Y.S. also received materials, equipment and gifts of drugs from CMG Pharmaceutical, Co., Ltd. (Seongnam, Korea). J.Y.S. also received proofreading services for manuscript from Wordvice Company (Seoul, Korea). H.A. received funding for provision of study materials from CHA Advanced Research Institute and CMG Pharmaceutical, Co., Ltd. (Seongnam, Korea). H.A. also received equipment, materials, drugs from CMG Pharmaceutical. S.K. received funding for provision of study materials from CHA Advanced Research Institute and CMG Pharmaceutical, Co., Ltd. (Seongnam, Korea). S.K. also received equipment, materials, drugs from CMG Pharmaceutical. The authors have no other conflicts of interest to declare.

Ethical Statement: The authors are accountable for all aspects of the work in ensuring that questions related to the accuracy or integrity of any part of the work are appropriately investigated and resolved. All animal experiments were performed with the approval of the Institutional Animal Care and Use Committee Guidelines of CHA(Christianity Humanism Academia) University (IACUC220188, Seongnam, Korea) and in conformity with the National Guidelines for the Care and Use of Laboratory Animals.

References

1. Araghi M, Mannani R, Heidarnejad Maleki A, et al. Recent advances in non-small cell lung cancer targeted therapy; an update review. Cancer Cell Int 2023;23:162.
2. Yuan M, Huang LL, Chen JH, et al. The emerging treatment landscape of targeted therapy in non-small-cell lung cancer. Signal Transduct Target Ther 2019;4:61.
3. Ríos-Hoyo A, Moliner L, Arriola E. Acquired Mechanisms of Resistance to Osimertinib-The Next Challenge. Cancers (Basel) 2022;14:1931.
4. Gomatou G, Syrigos N, Kotteas E. Osimertinib Resistance: Molecular Mechanisms and Emerging Treatment Options. Cancers (Basel) 2023;15:841.
5. Soria JC, Ohe Y, Vansteenkiste J, et al. Osimertinib in Untreated EGFR-Mutated Advanced Non-Small-Cell Lung Cancer. N Engl J Med 2018;378:113-25.
6. Lazzari C, Gregorc V, Karachaliou N, et al. Mechanisms of resistance to osimertinib. J Thorac Dis 2020;12:2851-8.
7. Sattler M, Mambetsariev I, Fricke J, et al. A Closer Look at EGFR Inhibitor Resistance in Non-Small Cell Lung Cancer through the Lens of Precision Medicine. J Clin Med 2023;12:1936.
8. Lu Y, Bian D, Zhang X, et al. Inhibition of Bcl-2 and Bcl-xL overcomes the resistance to the third-generation EGFR tyrosine kinase inhibitor osimertinib in non-small cell lung cancer. Mol Med Rep 2021;23:48.
9. Kim D, Bach DH, Fan YH, et al. AXL degradation in combination with EGFR-TKI can delay and overcome acquired resistance in human non-small cell lung cancer cells. Cell Death Dis 2019;10:361.
10. Tang Y, Zang H, Wen Q, et al. AXL in cancer: a modulator of drug resistance and therapeutic target. J Exp Clin Cancer Res 2023;42:148.

11. Song KA, Faber AC. Epithelial-to-mesenchymal transition and drug resistance: transitioning away from death. J Thorac Dis 2019;11:E82-5.
12. Celià-Terrassa T, Kang Y. How important is EMT for cancer metastasis? PLoS Biol 2024;22:e3002487.
13. Akhmetkaliyev A, Alibrahim N, Shafiee D, et al. EMT/MET plasticity in cancer and Go-or-Grow decisions in quiescence: the two sides of the same coin? Mol Cancer 2023;22:90.
14. Fu K, Xie F, Wang F, et al. Therapeutic strategies for EGFR-mutated non-small cell lung cancer patients with osimertinib resistance. J Hematol Oncol 2022;15:173.
15. Wang Q, Yang S, Wang K, et al. MET inhibitors for targeted therapy of EGFR TKI-resistant lung cancer. J Hematol Oncol 2019;12:63.
16. Coleman N, Hong L, Zhang J, et al. Beyond epidermal growth factor receptor: MET amplification as a general resistance driver to targeted therapy in oncogene-driven non-small-cell lung cancer. ESMO Open 2021;6:100319.
17. Xu L, Wang F, Luo F. MET-targeted therapies for the treatment of non-small-cell lung cancer: A systematic review and meta-analysis. Front Oncol 2022;12:1013299.
18. The Role of MET and c-Met in Advanced NSCLC (2023) Cancernetwork. July 21. Sponsored by AbbVie. Available online: https://www.cancernetwork.com/view/the-role-of-met-and-c-met-in-advanced-nsclc
19. Wang Y, Tian P, Xia L, et al. The clinical efficacy of combinatorial therapy of EGFR-TKI and crizotinib in overcoming MET amplification-mediated resistance from prior EGFR-TKI therapy. Lung Cancer 2020;146:165-73.
20. F Smit E, Dooms C, Raskin J, et al. INSIGHT 2: a phase II study of tepotinib plus osimertinib in MET-amplified NSCLC and first-line osimertinib resistance. Future Oncol 2022;18:1039-54.
21. Oxnard GR, Yang JC, Yu H, et al. TATTON: a multi-arm, phase Ib trial of osimertinib combined with selumetinib, savolitinib, or durvalumab in EGFR-mutant lung cancer. Ann Oncol 2020;31:507-16.
22. Sequist LV, Han JY, Ahn MJ, et al. Osimertinib plus savolitinib in patients with EGFR mutation-positive, MET-amplified, non-small-cell lung cancer after progression on EGFR tyrosine kinase inhibitors: interim results from a multicentre, open-label, phase 1b study. Lancet Oncol 2020;21:373-86.
23. Yang YM, Jang Y, Lee SH, et al. AXL/MET dual inhibitor, CB469, has activity in non-small cell lung cancer with acquired resistance to EGFR TKI with AXL or MET activation. Lung Cancer 2020;146:70-7.
24. Li W, Xiong X, Abdalla A, et al. HGF-induced formation of the MET-AXL-ELMO2-DOCK180 complex promotes RAC1 activation, receptor clustering, and cancer cell migration and invasion. J Biol Chem 2018;293:15397-418.
25. Lei T, Xu T, Zhang N, et al. Anlotinib combined with osimertinib reverses acquired osimertinib resistance in NSCLC by targeting the c-MET/MYC/AXL axis. Pharmacol Res 2023;188:106668.
26. Taniguchi H, Yamada T, Wang R, et al. AXL confers intrinsic resistance to osimertinib and advances the emergence of tolerant cells. Nat Commun 2019;10:259.
27. Choi YJ, Kim JH, Rho JK, et al. AXL and MET receptor tyrosine kinases are essential for lung cancer metastasis. Oncol Rep 2017;37:2201-8.
28. Riedel R, Fassunke J, Tumbrink HL, et al. Resistance to MET inhibition in MET-dependent NSCLC and therapeutic activity after switching from type I to type II MET inhibitors. Eur J Cancer 2023;179:124-35.
29. Fujino T, Kobayashi Y, Suda K, et al. Sensitivity and Resistance of MET Exon 14 Mutations in Lung Cancer to Eight MET Tyrosine Kinase Inhibitors In Vitro. J Thorac Oncol 2019;14:1753-65.
30. Fujino T, Mitsudomi T. Acquired Resistance Mechanism for MET Tyrosine Kinase Inhibitor. JTO Clin Res Rep 2021;2:100134.
31. Recondo G, Bahcall M, Spurr LF, et al. Molecular Mechanisms of Acquired Resistance to MET Tyrosine Kinase Inhibitors in Patients with MET Exon 14-Mutant NSCLC. Clin Cancer Res 2020;26:2615-25.
32. Piper-Vallillo AJ, Halbert BT, Rangachari D, et al. Acquired Resistance to Osimertinib Plus Savolitinib Is Mediated by MET-D1228 and MET-Y1230 Mutations in EGFR-Mutated MET-Amplified Lung Cancer. JTO Clin Res Rep 2020;1:100071.
33. Kang J, Chen HJ, Wang Z, et al. Osimertinib and Cabozantinib Combinatorial Therapy in an EGFR-Mutant Lung Adenocarcinoma Patient with Multiple MET Secondary-Site Mutations after Resistance to Crizotinib. J Thorac Oncol 2018;13:e49-53.
34. Bahcall M, Paweletz CP, Kuang Y, et al. Combination of Type I and Type II MET Tyrosine Kinase Inhibitors as Therapeutic Approach to Prevent Resistance. Mol Cancer Ther 2022;21:322-35.

Cite this article as: Song JY, An H, Kim S. A novel mesenchymal epithelial transition (MET) inhibitor, CB538, relieves acquired resistance in *EGFR*-mutated *MET*-amplified NSCLC. Transl Cancer Res 2025;14(3):1915-1927. doi: 10.21037/tcr-24-1614